Dynamic CT technique for assessment of wrist joint instabilities

Shuai Leng[a)]
Department of Radiology, Mayo Clinic College of Medicine, Rochester, Minnesota 55905

Kristin Zhao
Biomechanics Laboratory, Division of Orthopedic Research, Mayo Clinic College of Medicine, Rochester, Minnesota 55905

Mingliang Qu
Department of Radiology, Mayo Clinic College of Medicine, Rochester, Minnesota 55905

Kai-Nan An
Biomechanics Laboratory, Division of Orthopedic Research, Mayo Clinic College of Medicine, Rochester, Minnesota 55905

Richard Berger
Department of Orthopedic Surgery, Mayo Clinic College of Medicine, Rochester, Minnesota 55905

Cynthia H. McCollough
Department of Radiology, Mayo Clinic College of Medicine, Rochester, Minnesota 55905

(Received 1 September 2010; revised 21 November 2010; accepted for publication 6 January 2011; published 20 July 2011)

Purpose: To develop a 4D [three-dimensional (3D) + time] CT technique to capture high spatial and temporal resolution images of wrist joint motion so that dynamic joint instabilities can be detected before the development of static joint instability and onset of osteoarthritis (OA).
Methods: A cadaveric wrist was mounted onto a custom motion simulator and scanned with a dual source CT scanner during radial–ulnar deviation. A dynamic 4D CT technique was utilized to reconstruct images at 20 equidistant time points from one motion cycle. 3D images of carpal bones were generated using volume rendering techniques (VRT) at each of the 20 time points and then 4D movies were generated to depict the dynamic joint motion. The same cadaveric wrist was also scanned after cutting all portions of the scapholunate interosseus ligament to simulate scapholunate joint instability. Image quality were assessed on an ordinal scale (1–4, 4 being excellent) by three experienced orthopedic surgeons (specialized in hand surgery) by scoring 2D axial images. Dynamic instability was evaluated by the same surgeons by comparing the two 4D movies of joint motion. Finally, dose reduction was investigated using the cadaveric wrist by scanning at different dose levels to determine the lowest radiation dose that did not substantially alter diagnostic image quality.
Results: The mean image quality scores for dynamic and static CT images were 3.7 and 4.0, respectively. The carpal bones, distal radius and ulna, and joint spaces were clearly delineated in the 3D VRT images, without motion blurring or banding artifacts, at all time points during the motion cycle. Appropriate viewing angles could be interactively selected to view any articulating structure using different 3D processing techniques. The motion of each carpal bone and the relative motion among the carpal bones were easily observed in the 4D movies. Joint instability was correctly and easily detected in the scan performed after the ligament was cut by observing the relative motion between the scaphoid and lunate bones. Diagnostic capability was not sacrificed with a volume CT dose index ($CTDI_{vol}$) as low as 18 mGy for the whole scan, with estimated skin dose of approximately 33 mGy, which is much lower than the threshold for transient skin erythema (2000 mGy).
Conclusions: The proposed dynamic 4D CT imaging technique generated high spatial and high temporal resolution images without requiring periodic joint motion. Preliminary results from this cadaveric study demonstrate the feasibility of detecting joint instability using this technique. © *2011 American Association of Physicists in Medicine*. [DOI: 10.1118/1.3577759]

Key words: computed tomography, 4D CT, dynamic imaging, joint instability

I. INTRODUCTION

Osteoarthritis (OA) is one of the most pervasive disabling diseases in medicine today. This painful disease currently affects about 27 million Americans,[1,2] with an estimated cost three times the cost of rheumatoid arthritis,[3] with more than half of the costs due to the inability to work.[4] A prevailing explanation for the etiology of OA is joint instability or other abnormal motion of the articulating bony structures.

While static instabilities can be diagnosed using routine imaging techniques, dynamic instabilities do not demonstrate abnormalities on routine radiographic examinations, even though these patients continue to have disabling pain.[5] If physicians are able to diagnose dynamic joint instabilities prior to the development of significant OA, surgical intervention may restore normal function before the onset of arthritis or static deformities.[6–9] Here, we demonstrate the feasibility of a dynamic, three-dimensional (3D) measure of joint motion for the early detection of functional joint abnormalities.

Of the upper extremity joints, the wrist joint is the most susceptible to injury.[10] Instabilities of the wrist joint are characterized by subtle abnormalities in bony motion and are usually elicited during motion or in loaded conditions.[11,12] The scapholunate joint is an important carpal joint for wrist movement. Similar to the anterior cruciate ligament in the knee, the scapholunate interosseous ligament (SLIL) is considered the primary stabilizer of the scapholunate joint.[13] Injuries to the SLIL are the most frequent cause of carpal instability and account for a considerable degree of wrist dysfunction.[11] Patients with SLIL injuries may experience wrist pain or a snapping sensation in the joint with motion,[14,15] with no abnormalities in the scaphoid or lunate posture on static or stress radiographs.[6,7,16] Although fluoroscopy and biplanar fluoroscopy have been used for imaging the dynamic movement of joints when the movement occurs primarily about a single axis and when evaluating gross instabilities or abnormalities, the 2D nature of fluoroscopy limited its application in detecting complex and subtle musculoskeletal abnormalities, such as wrist joint instabilities.[17–24]

CT has been widely used in static wrist imaging to detect complex fractures, ligamentous injuries, and dislocations.[25,26] Compared with conventional radiography, CT has the advantage of generating three-dimensional images to display the complicated articulating structures in the wrist. Recently, the feasibility to evaluate wrist joint motion using 4D CT has been investigated by adopting a retrospectively gated technique similar to that used in ECG-gated cardiac CT.[27–32] Image slices corresponding to the same motion phase but different longitudinal positions were retrospectively sorted to form a 3D volume. Periodic motion was required to ensure that the moving organ (e.g., heart or wrist) returned to the same location for a given phase. Dynamic wrist imaging also has been implemented on a mobile C-arm system during periodic joint motion.[33,34] One limitation of the gated technique is that it requires periodic joint motion at the same frequency and magnitude, which is difficult to maintain in patients with pathology. Band artifacts are observed for imperfect periodic motion, similar to the band artifacts in cardiac CT scans with variable heart beat rate. Streak artifacts were also observed in the C-arm 4D joint imaging system due to undersampling and nonoptimal sampling patterns.[33,34]

Our goal is to detect joint instabilities while the wrist is moving freely, as in activities of daily living. Hence, a 4D CT technique without the requirement of periodic motion was used. A dynamic CT technique, similar to that used in CT perfusion, allowed for evaluation of wrist motion without the requirement of gating, and cadaveric studies were conducted to evaluate the feasibility of detecting wrist joint instability using this technique.

II. MATERIALS AND METHODS

II.A. Motion simulator and cadaveric specimen

A custom motion simulator was fabricated to generate radial–ulnar deviation at the wrist joint in a cadaveric forearm–hand specimen. Following approval by the Mayo Clinic Biospecimen committee, a cadaveric forearm-hand specimen was secured from the Anatomical Bequest program. We exposed the proximal ends of the radius and ulna bone in the cadaveric forearm and firmly mounted it to the device (Fig. 1). The hand was attached to an acrylic paddle via a single plastic screw through the second intermetacarpal space, just proximal to the deep intermetacarpal ligament. Two linear slides under the paddle provided composite motions in the x- and z-axes. A programmable stepper motor (Applied Motion Products, Watsonville, CA) produced belt-driven motion of the paddle along the x-axis, with free motion of the paddle in the z-axis. The motor was controlled by a controller/driver (ARCUS Technology, Inc., Livermore, CA) connected to a personal laptop in which different motion profiles could be programmed. In this study, it was programmed to allow the hand to perform radial-ulnar motion through an arc of 30° (10° of radial deviation and 20° of ulnar deviation). The wrist was programmed to move at 30°/s, representing a typical wrist motion speed.[35] The wrist was aligned in the CT scanner so that the center of the wrist was centered in the scan field of view (FOV) and no metal components were included in the primary beam. A standard CT scan of the static wrist (without motion) was also conducted for image quality comparison with dynamic CT.

Experiments were also conducted in the cadaveric wrist to demonstrate the capability of the proposed 4D CT imaging to detect joint instability. Scapholunate joint instability was simulated in the cadaveric specimen by cutting all

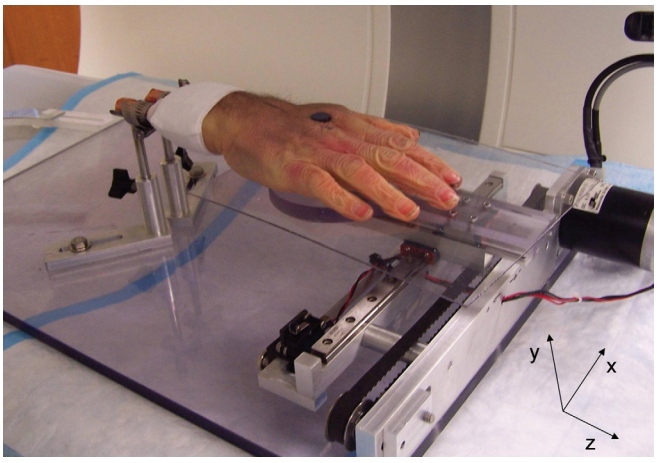

FIG. 1. A cadaveric forearm and hand mounted on a custom fabricated motion simulator producing motion along the x-axis.

portions of the scapholunate interosseus ligament (dorsal, proximal, and volar). The same motion profile and scanning techniques (presented below) used in the intact wrist scan were utilized during the imaging of the wrist after ligament sectioning.

II.B. Dynamic 4D CT imaging protocol

Because imperfect periodicity, which is likely in patient studies, generates banding artifacts in retrospectively gated techniques, a dynamic sequential scanning mode without gating, similar to that in CT perfusion, was investigated in this study. In this scanning mode, projection data of the moving wrist are continuously acquired without table translation. Data acquisition is completed after a single motion cycle, in contrast to the gated 4D CT, in which repeated wrist motion is required. Three-dimensional renderings of the wrist could be reconstructed at any temporal increment throughout the motion cycle. Since only one motion cycle is required for data acquisition, periodic motion is not required and band artifacts are avoided.

II.C. CT scanner, scanning and reconstruction parameters

The cadaveric wrist was scanned using a dual source CT scanner (Definition Flash, Siemens Healthcare, Forchheim, Germany). This scanner is equipped with two x-ray tubes and two detector systems with angular offset of 94°.[36] The two 64 row detectors, with 0.6 mm for each detector cell, provide a longitudinal coverage of 38.4 mm. A rotation time of 0.28 s provided a temporal resolution of 75 ms using the dual source scanning mode. This is an improvement in temporal resolution over that from single source CT scanners by more than a factor of 2.[36] Temporal resolution is critical in 4D CT wrist imaging to avoid image degradation due to motion blurring. Together with the 0.6 mm isotropic spatial resolution, this scanner appears to meet the high spatial resolution and high temporal resolution requirements of 4D CT wrist imaging.[28]

The 4D CT dynamic wrist imaging requires continuous data acquisition at a fixed table position using dual source scan mode (75 ms temporal resolution). As no appropriate dual source perfusion protocol was available, a dual source sequential cardiac scanning protocol was modified to accommodate the need. An external ECG simulator was connected to the scanner to generate ECG signals, which were required for the cardiac-based scan protocol. Heart rate was adjusted to be 30 bpm so that the time of one cardiac cycle was 2 s, the same as the wrist motion cycle time. Data were acquired over one motion cycle (2 s) without any table translation. The ECG signals were used in this study solely to satisfy the existing (cardiac) scan protocol so that it could be used for our purpose. They were not used in the image reconstruction. Tube potential was 140 kV and the tube-current time-product was 200 mAs per rotation, which corresponded to a total $CTDI_{vol}$ of 110 mGy for the 2 s acquisition.

Images were reconstructed using the dual source reconstruction algorithm commercially implemented on the scanner. An image matrix of 512 × 512 was used with 150 mm scan FOV, which covered the cross-section of the wrist. The reconstructed image thickness was 0.6 mm with an overlapped reconstruction increment of 0.3 mm. Both a medium sharp (B40) and a sharp (B70) reconstruction kernel were used for each image reconstruction. The motion cycle was divided into 20 equivalent time points, and images were reconstructed at each time point. These 20 time points represented 20 phases of one radioulnar deviation cycle, with the neutral position defined as 0% phase.

Reconstructed images were postprocessed using commercial software (Syngo, Siemens Healthcare, Forchheim, Germany) to generate 3D and 4D images. Volume rendering techniques (VRT) were used to generate 3D images of carpal bones at each of the 20 phases. With these 3D images, a 4D movie was generated to demonstrate the dynamic motion of the cadaveric wrist.

II.D. Dose estimation and reduction

There has been some concern regarding the radiation dose associated with CT scans.[37] For scans of the wrist, stochastic effects are generally not a concern, as there are no radiosensitive organs inside or near the scan field of view. To evaluate whether deterministic effects may be a concern, skin dose was estimated for the dynamic sequential scans based upon $CTDI_{vol}$ obtained from the scanner console using an established relationship between skin dose and $CTDI_{vol}$ taking into account patient size.[38] This estimated skin dose was compared with published thresholds for skin effects. We also investigated the potential to reduce dose by scanning the cadaveric wrist at different dose levels (140 kV and 200 mAs per rotation, and 120 kV and 50 mAs per rotation).

II.E. Image quality evaluation and joint instability detection

The reconstructed 2D axial images from a standard CT scan of the static wrist and from a dynamic CT scan of the moving wrist were shown to three experienced orthopedic surgeons (specialized in hand surgery) for image quality evaluation. They were asked to score these images with a 4 point system: 1 = noninterpretable; 2 = possibly interpretable with strong image artifacts, poor signal to noise ratio; 3 = interpretable with minimal image artifacts and sufficient signal to noise ratio; and 4 = interpretable without image artifacts.[39]

For wrist instability evaluation, 4D movies of the intact wrist and the wrist after the ligament was cut were presented to the same orthopedic surgeons side by side for a blinded review. The surgeons were asked to identify which scan, if any, demonstrated joint instability. For scans at different dose levels, 2D axial and 3D VRT images at the original dose level (140 kVp, 200 mAs per rotation) and reduced dose level (120 kVp, 50 mAs per rotation) were presented together to subjectively determine the lowest acceptable dose levels that did not comprise the confidence of the diagnosis of joint instability.

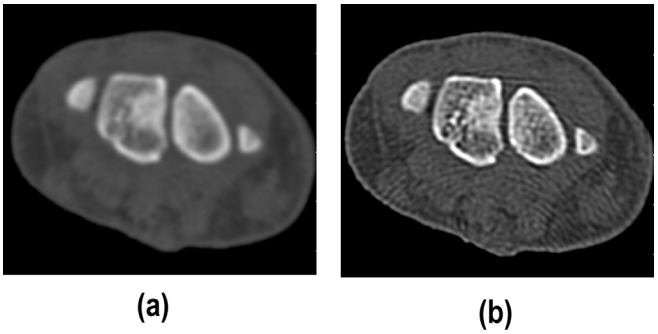

FIG. 2. Images reconstructed using a medium sharp kernel [B40 (a)] and a sharp kernel [B70 (b)], with display window width of 2000 HU and window level of 500 HU.

III. RESULTS

Sample axial images at 60% phase were reconstructed using a medium sharp kernel (B40) and a sharp kernel (B70) as shown in Fig. 2. As expected, images using the medium sharp kernel had lower noise than those using a sharp kernel, while those from the sharp kernel had better spatial resolution. All three surgeons scored 2D image slices from static CT scans as 4 (interpretable without image artifacts). Two of them scored 2D image slices from dynamic CT scans as 4 and the other one scored them as 3 (as interpretable with minimal image artifacts and sufficient signal to noise ratio).

The 3D VRT images for all phases were generated in which the carpal bones, distal radius and ulna, and joint spaces were without motion blurring or banding artifacts (Fig. 3). 4D movies allowed the surgeons to visualize the motion of each carpal bone and the change in joint space throughout the motion cycle (movie file included in supplementary materials).[40] Use of interactive visualization software allowed the carpal bones and joint motion to be visualized from any arbitrary viewing angle, interactively selecting the best angle(s) with which to view articulating structures. For example, a palmar view best showed overall wrist motion for all carpal bones [Figs. 3(a)–(c)], while radial views were most useful in evaluating scaphoid motion [Figs. 3(d)–(f)]. Virtual radiographs provided the surgeons with images similar to traditional radiographic images (Fig. 4).

For scans after the ligament was cut, the same postprocessing was conducted and 3D VRT images and 4D movies were generated and compared with the scans of the intact wrist. Figure 5 shows the comparison between these two scans using VRT images at different positions. For the intact (normal) wrist, the scaphoid and lunate carpal bones moved together during the joint motion and there was no relative motion between these two bones. However, after the ligament was cut, relative motion between the scaphoid and lunate was observed during the radial-ulnar deviation, indicating joint instability. This different motion pattern (translation and rotation) between the normal wrist and the one with joint instability was clearly demonstrated in the 4D movie (included as supplementary materials).[40] All three orthopedic surgeons correctly identified the scapholunate instability in the wrist with the cut ligament without any hesitation.

The $CTDI_{vol}$ of the full-dose scan (140 kVp, 200 mAs per rotation, 2 s scan time) was 110 mGy and the skin dose was estimated to be approximately 200 mGy given the small size of the wrist, which is a factor of 10 lower than the minimum threshold for skin effects (2000 mGy).[41] Therefore, no deterministic skin injury would be expected. Potential cancer risk is similarly negligible because of the small exposure volume and insensitivity of the exposed tissues to radiation. For scans at reduced dose level, all three surgeons indicated that images obtained using 120 kVp and 50 mAs per rotation ($CTDI_{vol}$ = 18 mGy) had sufficient image quality and did not compromise their diagnostic confidence (Fig. 6). This afforded the potential for a factor of 6 reduction in dose (skin dose of 33 mGy).

IV. DISCUSSION AND CONCLUSION

In this study, we have proposed a dynamic 4D CT imaging method to detect joint motion and demonstrated our methods using a cadaveric wrist and a custom motion simulator. This technique generated high spatial and temporal resolution (75 ms) images of the joint on the dual source CT scanner. As no periodic motion was required, the potential for banding artifacts from gated techniques was eliminated. This cadaveric study demonstrated the difference in motion patterns (translation and rotation) between normal and abnormal (with joint instability) wrists using this proposed

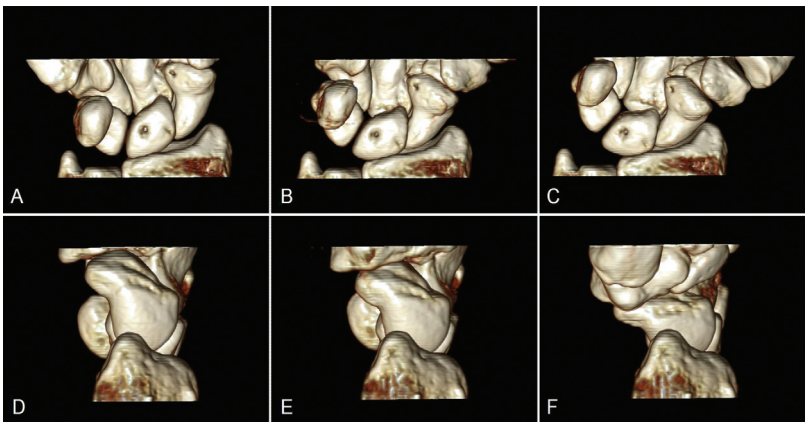

FIG. 3. Volume-rendered images (top row: palmar view; bottom row: radial view) of a cadaver wrist scanned with a dynamic scanning mode on a dual source CT scanner. Images in ulnar deviation (a, d), neutral (b, e), and radial deviation (c, f) positions show individual carpal bones and joint spaces clearly in three dimensions.

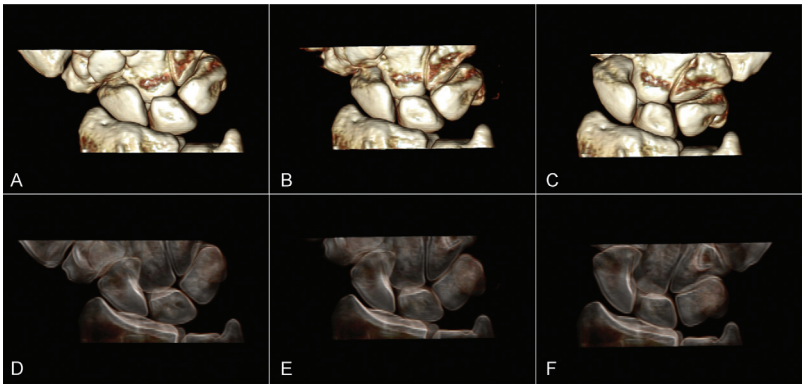

FIG. 4. Volume-rendered images (top row, dorsal view) and virtual radiography images (bottom row) of the cadaveric wrist at radial deviation (a, d), neutral (b, e), and ulnar deviation positions (c, f).

4D CT technique. Radiation dose from this technique was much lower than the threshold for deterministic effects, and stochastic risk was extremely low due to the absence of critical organs. Since no table translation was involved in this dynamic CT scanning mode, the longitudinal coverage of the wrist was limited to the detector size along the z-axis (rotation axis of the scanner), which was 38.4 mm on the dual source scanner used in this study. This coverage is sufficient for imaging small joints like the wrist, especially for the purpose of scapholunate instability evaluation, where the proximal carpal bones are of major interest. Z-axis coverage is not a fundamental limitation of this mode, however, as scanners with up to a 16-cm detector width have been used for normal wrist and knee dynamic imaging.[39] However, the temporal resolution of the wide detector, single source scanner was limited to 500 ms; it was 75 ms for the dual source CT scanner used in our study. Due to the better temporal resolution, the wrist joint was able to be moved at speeds similar to those of daily activities (2 s per cycle, compared with 10 s per cycle in Ref. 39) without generating motion artifacts. Besides the intact normal wrist, we have also imaged a wrist with a scapholunate instability and demonstrated the feasibility to detect these instabilities using our technique.

In clinical practice, physicians can make diagnoses based upon the qualitative evaluation of joint motion. However, to quantify subtle dynamic joint instabilities requires quantitative kinematic analysis, which involves a series of image processing procedures and computations, e.g., image

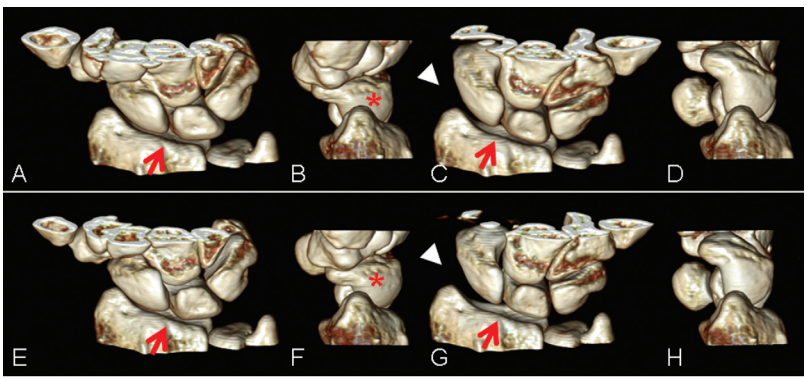

(a)

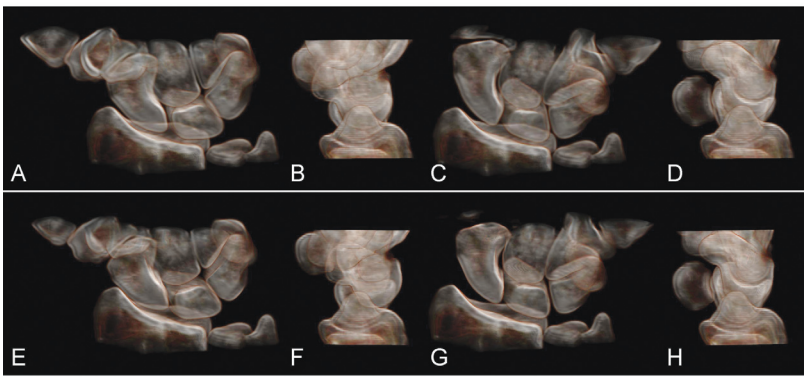

(b)

FIG. 5. (a) Volume-rendered images of a normal wrist (top row) and the wrist after the scapholunate interosseous ligament was cut (bottom row), in radial (A, B and E, F) and ulnar (C, D and G, H) deviation phases during dynamic motion. Both dorsal (A, C and E, G) and radial views (B, D and F, H) demonstrated the deviation, flexion and extension of both the scaphoid and lunate for comparison between the normal and injured wrist. Dissociated motion of the scaphoid and lunate (arrows) can be visualized at both phases in the dorsal views (E and G). Over-flexion of scaphoid (asterisk) during radial deviation in the radial view (F) and increased scapholunate and radioscaphoid distance (arrowheads) during ulnar deviation in dorsal view can be clearly visualized. (b) Volume-rendered images that mimic fluoroscopic images can also be used to better visualize the intercarpal positioning and relative motions.

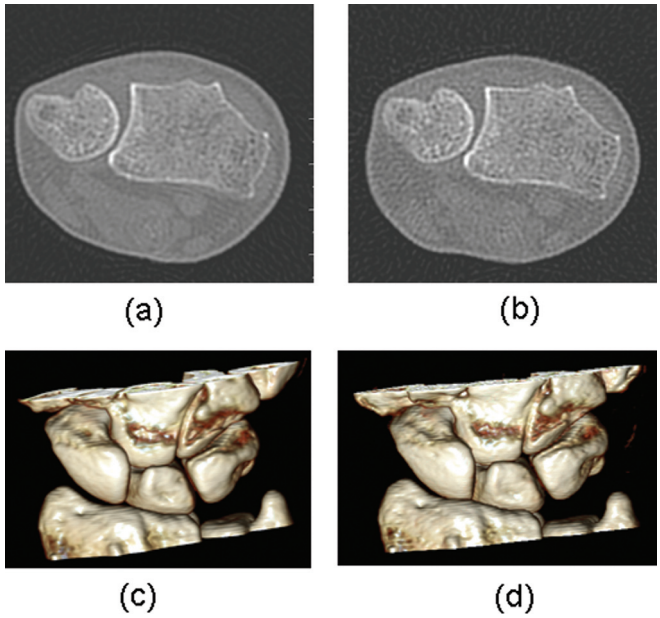

FIG. 6. Axial images and volume-rendered images from scans with 140 kV, 200 mAs per rotation [$CTDI_{vol}$ = 110 mGy (a) and (c)] and 120 kV, 50 mAs per rotation [$CTDI_{vol}$ = 18 mGy (b) and (d)]. Sufficient image quality is maintained in the low dose scan [(b) and (d)] to diagnose join instability with confidence.

segmentation and registration. Ongoing research in our group is focused on developing software to automatically generate kinematic data to assist with clinical diagnoses. These quantitative data can also be used to compile a database for normal wrist kinematics and kinematics for wrists with joint instabilities.

In conclusion, a 4D CT technique was used to detect joint instability in a cadaveric wrist. Image quality assessment demonstrated that similar image quality was achieved for dynamic CT compared with static CT. Human observer evaluation demonstrated the feasibility of this method to detect wrist joint instability.

ACKNOWLEDGMENTS

This work is partially supported by a Mayo Novel Methodology Award [Grant No. 1 UL1 RR024150, National Center for Research Resources (NCRR), a component of the National Institutes of Health (NIH) and the NIH Roadmap for Medical Research], an NIH grant, Grant No. R21 AR057902, and a Mayo Clinic Radiology Department seed fund. The authors would like to thank Lawrence J. Berglund for his assistance in motion simulator fabrication and Kris Nunez for her assistance in manuscript preparation.

[a]Author to whom correspondence should be addressed. Electronic mail: leng.shuai@mayo.edu

[1]R. C. Lawrence *et al.*, "Estimates of the prevalence of arthritis, selected musculoskeletal disorders in the United States," Arthritis Rheum. **41**, 778–799 (1998).
[2]C. G. Helmick *et al.*, "Estimates of the prevalence of arthritis and other rheumatic conditions in the United States. Part I," Arthritis Rheum. **58**, 15–25 (2008).
[3]E. Yelin, "The economics of osteoarthritis," (Osteoarthritis, Oxford University Press, New York, 1998), pp. 23–30.
[4]D. T. Felson and Y. Zhang, "An update on the epidemiology of knee and hip osteoarthritis with a view to prevention," Arthritis Rheum. **41**, 1343–1355 (1998).
[5]F. W. Werner, W. H. Short, and J. K. Green, "Changes in patterns of scaphoid and lunate motion during functional arcs of wrist motion induced by ligament division," J. Hand Surg. [Am] **30**, 1156–1160 (2005).
[6]B. D. Adams and R. A. Berger, "An anatomic reconstruction of the distal radioulnar ligaments for posttraumatic distal radioulnar joint instability," J. Hand Surg. [Am] **27**, 243–251 (2002).
[7]B. Bickert, M. Sauerbier, and G. Germann, "Scapholunate ligament repair using the Mitek bone anchor," J. Hand Surg. [Br] **25**, 188–192 (2000).
[8]L. C. Teoh and A. K. Yam, "Anatomic reconstruction of the distal radioulnar ligaments: Long-term results," J. Hand Surg. [Br] **30**, 185–193 (2005).
[9]J. J. Walsh, R. A. Berger, and W. P. Cooney, "Current status of scapholunate interosseous ligament injuries," J. Am. Acad. Orthop. Surg. **10**, 32–42 (2002).
[10]B. Anderson, *Office Orthopedics for Primary Care: Diagnosis Treatment*, 2nd ed. (WB Saunders Company, Philadelphia, 1999).
[11]R. L. Linscheid *et al.*, "Traumatic instability of the wrist. Diagnosis, classification, and pathomechanics," J. Bone. Joint Surg. Am. **54**, 1612–1632 (1972).
[12]H. Watson *et al.*, "Rotary subluxation of the scaphoid: A spectrum of instability," J. Hand Surg. [Br] **18**, 62–64 (1993).
[13]R. A. Berger, "The ligaments of the wrist. A current overview of anatomy with considerations of their potential functions," Hand Clin. **13**, 63–82 (1997).
[14]F. M. Howard, T. Fahey, and E. Wojcik, "Rotatory subluxation of the navicular," Clin. Orthop. Relat. Res. **104**, 134–139 (1974).
[15]W. T. Jackson and J. M. Protas, "Snapping scapholunate subluxation," J. Hand Surg. [Am] **6**, 590–594 (1981).
[16]H. K. Watson and D. M. Black, "Instabilities of the wrist," Hand Clin. **3**, 103–111 (1987).
[17]M. J. Bey *et al.*, "Validation of a new model-based tracking technique for measuring three-dimensional in vivo glenohumeral joint kinematics," J. Biomech. Eng. **128**, 604–609 (2006).
[18]J. W. Fernandez *et al.*, "Integrating modelling, motion capture, x-ray fluoroscopy to investigate patellofemoral function during dynamic activity," Comput. Methods Biomech. Biomed. Eng. **11**, 41–53 (2008).
[19]T. W. Lu *et al.*, "In vivo three-dimensional kinematics of the normal knee during active extension under unloaded, loaded conditions using single-plane fluoroscopy," Med. Eng. Phys. **30**, 1004–1012 (2008).
[20]M. R. Mahfouz *et al.*, "In vivo assessment of the kinematics in normal, anterior cruciate ligament-deficient knees," J. Bone Jt. Surg., Am. **86**, 56–61 (2004).
[21]N. Nishinaka *et al.*, "Determination of in vivo glenohumeral translation using fluoroscopy, shape-matching techniques," J. Shoulder Elbow Surg. **17**, 319–322 (2008).
[22]M. Tamaki *et al.*, "In vivo kinematic analysis of a high-flexion posterior stabilized fixed-bearing knee prosthesis in deep knee-bending motion," J. Arthroplasty **23**, 879–885 (2008).
[23]S. Tashman and W. Anderst, "In-vivo measurement of dynamic joint motion using high speed biplane radiography and CT: Application to canine ACL deficiency," J. Biomech. Eng. **125**, 238–245 (2003).
[24]S. Wang *et al.*, "Measurement of vertebral kinematics using noninvasive image matching method-validation and application," Spine **33**, E355–E361 (2008).
[25]R. Nakamura *et al.*, "Three-dimensional CT imaging for wrist disorders," J. Hand Surg. [Br] **14**, 53–58 (1989).
[26]B. W. Hindman *et al.*, "Occult fractures of the carpals and metacarpals: Demonstration by CT," AJR Am. J. Roentgenol. **153**, 529–532 (1989).
[27]E. Baltali, A. Primak, M. Koff, B. Schmidt, K. D. Zhao, and C. McCollough, "4D CT Imaging of the temporomandibular joint: Feasibility in a cadaveric specimen," *Radiology Society of North America*, Chicago, IL (2007).
[28]S. Tay *et al.*, "Understanding the relationship of image quality and motion velocity in gated-CT imaging: Preliminary work for 4D musculoskeletal imaging," JCAT **32**, 634–639 (2008).

[29]S. C. Tay *et al.*, "Four-dimensional computed tomographic imaging in the wrist: proof of feasibility in a cadaveric model," Skeletal Radiol. **36**, 1163–1169 (2007).
[30]M. Kachelriess and W. A. Kalender, "Electrocardiogram-correlated image reconstruction from subsecond spiral computed tomography scans of the heart," Med. Phys. **25**, 2417–2431 (1998).
[31]B. Ohnesorge *et al.*, "Cardiac imaging by means of electrocardiographically gated multisection spiral CT: Initial experience," Radiology **217**, 564–571 (2000).
[32]K. Taguchi and H. Anno, "High temporal resolution for multislice helical computed tomography," Med. Phys. **27**, 861–872 (2000).
[33]B. Carelsen *et al.*, "4D rotational x-ray imaging of wrist joint dynamic motion," Med. Phys. **32**, 2771–2776 (2005).
[34]B. Carelsen *et al.*, "Detection of in vivo dynamic 3-D motion patterns in the wrist joint," IEEE. Trans. Biomed. Eng. **56**, 1236–1244 (2009).
[35]W. Marras, "Wrist motions in industry," Ergonomics **36**, 341–351 (2003).
[36]T. G. Flohr *et al.*, "Dual-source spiral CT with pitch up to 3.2 and 75 ms temporal resolution: Image reconstruction and assessment of image quality," Med. Phys. **36**, 5641–5653 (2009).
[37]D. J. Brenner and E. J. Hall, "Computed tomography—An increasing source of radiation exposure," N. Engl. J. Med. **357**, 2277–2284 (2007).
[38]S. Leng, T. Vrieze, L. Yu, and C. McCollough "Skin Dose Estimation from CT Perfusion Studies: Influence of Patient Size, Beam Collimation and Scanner Type," Radiology Society of North America, Chicago, IL (2010).
[39]V. Kalia *et al.*, "Functional joint imaging using 256-MDCT: Technical feasibility," AJR Am. J. Roentgenol. **192**, W295–W299 (2009).
[40]See supplementary material at E-MPHYA6-38-035105 for 4D movies of the normal wrist (normal_wrist.wmv) and a comparison between normal wrist and the one with joint instability (compare_normal_and_instaility.wmv).
[41]M. S. Stecker *et al.*, "Guidelines for patient radiation dose management," J. Vasc. Interv. Radiol. **20**, S263–S273 (2009).